Accepted Manuscript

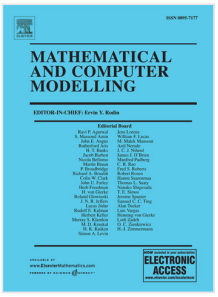

Analysis of a molecular structured population model with possible polynomial growth for the cell division cycle

Fadia Bekkal Brikci, Jean Clairambault, Benoît Perthame

PII: S0895-7177(07)00203-8
DOI: 10.1016/j.mcm.2007.06.008
Reference: MCM 3143

To appear in: *Mathematical and Computer Modelling*

Received date: 11 January 2007
Accepted date: 21 June 2007

Please cite this article as: F.B. Brikci, J. Clairambault, B. Perthame, Analysis of a molecular structured population model with possible polynomial growth for the cell division cycle, *Mathematical and Computer Modelling* (2007), doi:10.1016/j.mcm.2007.06.008

Analysis of a molecular structured population model with possible polynomial growth for the cell division cycle

Fadia Bekkal Brikci, * Jean Clairambault, * Benoît Perthame*

We analyse both theoretically and numerically a nonlinear model of the dynamics of a cell population divided into proliferative and quiescent compartments that is described in [8]. It is a physiological age and molecule-structured population model for the cell division cycle, which aims at representing both healthy and tumoral tissues. A noticeable feature of this model is to exhibit tissue homeostasis for healthy tissue and unlimited growth for tumoral tissue. In particular, the present paper analyses model parameters for which a tumoral tissue exhibits polynomial growth and not mere exponential growth. Polynomial tumour growth has been recently advocated by several authors, on the basis either of experimental observations or of individual cell-based simulations which take space limitations into account. This model is able to take such polynomial growth behaviour into account without considerations on space, by proposing exchange functions between the proliferative and quiescent compartments.
Keywords: Cell division cycle, Structured population equations, Entropy method, Eigenelements.

1. Introduction: the model

A variety of structured cell population models has been studied by several authors [3,19,26,23], who analysed their interesting mathematical properties. In [4,18,19,36], the asynchronous exponential growth property was shown for a structured cell population model with proliferative and quiescent compartments. Our goal here is to design a generic cell population model applicable to the growth of both cancer and normal tissues, each of them comprising proliferative and quiescent compartments. The proliferative compartment represents the complete cell cycle which consists of four phases called G_1, S, G_2, M. The progression of a cell through these phases is controlled by various proteins, in particular cyclins and cyclin dependent kinases (CDKs). Recent measurements [21] indicate that *cyclins/CDKs* complexes are the most determinant control molecules for phase transitions, and each phase has its specific *cyclins/CDKs* complexes. Thus, in [8], we proposed to structure our cell population model by age and *cyclin/CDK* content.

Let $p(t,a,x)$and $q(t,a,x)$ be the densities of proliferating and quiescent cells, respectively, at time t with age a and content x in *cyclin D/(CDK4 or 6)* which is an important complex to control the transition between proliferation and quiescence. Then, the authors

*Institut de Recherche en Informatique et en Automatique, BP 105, F78153 Rocquencourt, France. Fadia.Bekkal_Brikci@inria.fr, Jean.Clairambault@inria.fr, Benoit.Perthame@ens.fr

in [8] derive the nonlinear system:

$$\begin{cases} \dfrac{\partial}{\partial t}p\left(t,a,x\right)+\dfrac{\partial}{\partial a}\left(\Gamma_0 p\left(t,a,x\right)\right)+\dfrac{\partial}{\partial x}\left(\Gamma_1\left(a,x\right)p\left(t,a,x\right)\right)= \\ \qquad\qquad -\left[L\left(a,x\right)+F(a,x)+d_1\right]p\left(t,a,x\right)+G\left(N\left(t\right)\right)q\left(t,a,x\right), \\ \dfrac{\partial}{\partial t}q\left(t,a,x\right)=L\left(a,x\right)p\left(t,a,x\right)-\left[G\left(N\left(t\right)\right)+d_2\right]q\left(t,a,x\right), \end{cases} \tag{1}$$

together with the following condition at the boundary $a=0$:

$$p\left(t,0,x\right)=\frac{2}{\Gamma_0}\int_0^{+\infty}\int_0^{+\infty}f\left(a,x,y\right)p\left(t,a,y\right)dady. \tag{2}$$

This is a physiological age and molecule-structured population model for the cell division cycle. Proliferating cells grow and divide whereas quiescent cells are assumed to be halted in their individual physiological evolution, in the sense that once a cell becomes quiescent, its age and cyclin content are fixed at their last values as belonging to a proliferative cell. In this way, quiescent cells do not age and do not change their cyclin content.

We denote here by Γ_0 the ratio between physiological and chronological time (a constant in what follows) and by $\Gamma_1\left(a,x\right)$ the evolution speed of *cyclin D/(CDK4 or 6)* with respect to physiological age. Following the derivation in [8], it is given by

$$\frac{\Gamma_1\left(a,x\right)}{\Gamma_0}=c_1\frac{x}{1+x}\left(\frac{c_3}{c_4}+e^{-c_4 a}w_1\right)-c_2x, \tag{3}$$

where c_1, c_3 are interpreted as synthesis rates and c_2, c_4 as degradation rates of the protein forming the complex and it is natural to assume that $w_1\leq\dfrac{c_3}{c_4}$ and

$$x_{\max}=\frac{c_1c_3}{c_2c_4}-1>0, \tag{4}$$

Therefore, a fundamental property of the characteristics in equation (3) is that the cyclin concentration x is upper limited by $x_{\max}$ when departing from a value less than $x_{\max}$. Because Γ_1 vanishes at $x=0$ there is no need of boundary condition at $x=0$.

Exits from the quiescent and the proliferative compartment are due either to apoptosis (physiological cell death) at rates d_1 and d_2, respectively, or to transition from the quiescent to the proliferative phase and vice versa. Here, we assume that the transition from proliferation to quiescence depends on age and cyclin content of the cell. At the beginning of the cell cycle, the cell remains in the proliferative phase but from a certain age on, if its content in *cyclin D/(CDK4 or 6)* is not high enough, the cell passes to the quiescent phase. We set the "demobilisation" (or "leak") function from proliferation to quiescence as:

$$L\left(a,x\right)=A_1\frac{A_2^{\gamma_2}}{A_2^{\gamma_2}+x^{\gamma_2}}\mathbb{1}_{[\bar{A},+\infty[}(a).$$

(where $\mathbb{1}_J$ denotes the indicator function of interval J). In this setting, if the Hill exponent γ_2 is high enough (e.g. between 5 and 10), A_2 is the "switching" cyclin content value x beyond which, the "leak" function L becoming close to zero (no more escape to quiescence), a cell population is irreversibly committed to process in the proliferating phase until division.
The reverse transition from quiescence to proliferation represented by the "recruitment" (or "getting in the cycle") function G is assumed to depend on the total weighted population of cells N (as in [27]). But more precisely in the present model, it depends on those cells that are qualified to be sensitive to environmental factors such as growth and anti-growth factors. If these factors acting on the populations of proliferating (p) and quiescent (q) cells are represented by the weights φ^* and ψ^*, respectively, then N will be defined by:

$$N(t) = \int_0^{+\infty}\int_0^{+\infty} \left[\varphi^*(a,x)p(t,a,x) + \psi^*(a,x)q(t,a,x)\right] dadx. \tag{5}$$

Two cases are studied in this paper, since we assume healthy tissues and tumours to behave differently with respect to the recruitment function G which always takes the form of a monotone decreasing (we have in mind population density inhibition) Hill function:

$$G(N) = \frac{\alpha_1\theta^n + \alpha_2 N^n}{\theta^n + N^n}, \qquad 0 < \alpha_2 < \alpha_1. \tag{6}$$

For the two cases we assume that the population grows when $N = 0$ (see section 2.2.1 below). According to (6), for N large, the fraction of the quiescent cells that reenter the proliferative phase decreases to α_2
1) For a healthy tissue, this fraction α_2 is not enough to maintain a growth, and the population decreases for the linear problem with $G = \alpha_2$,
2) For a tumour, this fraction α_2 sustains a growth of the system.

The distribution of the molecular material between daughter cells is assumed to be unequal (as in [23]): we consider that the distribution of the amount of *cyclin D/(CDK4 or 6)* between the two daughter cells is given by the conditional density $f(a,x,y)$ when they are born from a mother cell with content y in *cyclin D/CDK(4 or 6)*. From this interpretation, f has the following properties:

$$\begin{cases} f(a,x,y) &= 0 \quad \text{if } x > y, \\ f(a,x,y) &= f(a,y-x,x). \end{cases} \tag{7}$$

Then the fraction $F(a,y)$ of cells which at age a and content y leave the proliferating phase to undergo cell division - disappearing and being replaced by two daughter cells - is defined by:

$$F(a,y) = \int_0^{+\infty} f(a,x,y)dx.$$

Finally, in order to impose the conservation of total molecular content we need to impose

$$yF(a,y) = 2\int_0^{+\infty} xf(a,x,y)dx.$$

We choose for F a standard Hill function:

$$F(a,y) = \frac{k_1 y^{\gamma_1}}{k_2^{\gamma_1} + y^{\gamma_1}} \mathbb{1}_{[A^*,+\infty[}(a),$$

where k_1 is the maximum effect of *cyclin D* on cell division, k_2 is the cyclin content yielding its half-maximum effect, γ_1 is the Hill coefficient tuning the steepness of the switch at $y = k_2$ between 0 and k_1 for the effect, and A^* is the minimal cell cycle duration.

We also consider two cases for the cyclin repartition after division. The first choice is a uniform repartition

$$f(a,x,y) = \frac{F(a,y)}{y} \mathbb{1}_{[0,y]}(x). \tag{8}$$

The second choice is equal repartition in twice $x = y/2$

$$f(a,x,y) = F(a,y)\,\delta(x = \frac{y}{2}) \tag{9}$$

To complete system (1)–(2), we specify initial conditions,

$$p(0,a,x) = p_i(a,x) \geq 0, \quad q(0,a,x) = q_i(a,x) \geq 0, \qquad a \geq 0,\ x \geq 0, \tag{10}$$

where p_i and q_i are given functions such that N_i defined as in (5) is finite.

We then analyse the qualitative behaviour of the model, which enables us to distinguish a healthy tissue from a tumour by the asymptotic behaviour of their cell densities. One of the purposes of this paper is to show that tumoral growth is not restricted to exponential behaviour. In particular, our model is rich enough to be made compatible with experiments and individual based model simulations that exhibit polynomial growth [9,15].

2. Analysis and qualitative behaviour

We now perform the analysis of the model developed above. We use for this purpose the method of Generalised Relative Entropy (GRE), which was recently introduced in [28–30]. A general presentation of the method can be found in [33]. It allows us to deal with the model in its full generality. The GRE method is based on the study of eigenproblems for linearised systems and relies on the Krein-Rutman theorem for compact positive operators, see [14]. Other methods are possible, for instance methods based on the theory of abstract semigroups (but at any rate structural conditions as below are needed), or, in special cases, reduction to differential equations with delay (see [1] for instance).

2.1. Linear problem

The linear problem associated with (1) assumes that the transition rate from the quiescent to the proliferative state is a constant $\tilde{G}$, such that:

$$\begin{cases} \dfrac{\partial p}{\partial t} + \dfrac{\partial \left(\Gamma_0 p\right)}{\partial a} + \dfrac{\partial \left(\Gamma_1 \left(a,x\right) p\right)}{\partial x} = -\left(L\left(a,x\right) + F(a,x) + d_1\right) p\left(t,a,x\right) + \tilde{G} q\left(t,a,x\right), \\ \dfrac{\partial q}{\partial t} = L\left(a,x\right) p\left(t,a,x\right) - \left(\tilde{G} + d_2\right) q\left(t,a,x\right), \\ p\left(t,0,x\right) = \dfrac{2}{\Gamma_0} \int\limits_0^{+\infty} \int\limits_0^{+\infty} f\left(a,x,y\right) p(t,a,y) da dy. \end{cases} \tag{11}$$

Gyllenberg and Webb, studying a similar linear problem with simpler boundary conditions which allow for explicit formulas, by methods relying on the theory of continuous semigroups, proved the existence and uniqueness of a positive solution for the system, and also proved that it has the property of asynchronous exponential growth [18]. More generally, note that existence of weak solutions results in fact from variants of the Krein-Rutman theorem ([14]) but specific arguments for compactness are always needed. For the case at hand, the results in [29,33] will do.

Our analysis relies on the following conclusion: the growth rate associated with (11) -the so-called Malthus parameter- i.e., the first eigenvalue of the problem (also referred to as the Perron eigenvalue in the finite-dimensional case), is defined as the only λ yielding a nonnegative steady state (P,Q) solution to the system:

$$\begin{cases} \lambda P + \dfrac{\partial \left(\Gamma_0 P\right)}{\partial a} + \dfrac{\partial \left(\Gamma_1 \left(a,x\right) P\right)}{\partial x} = -\left(L\left(a,x\right) + F(a,x) + d_1\right) P + \tilde{G} Q, \\ \left(\lambda + \tilde{G} + d_2\right) Q = L\left(a,x\right) P, \\ P(0,x) = \dfrac{2}{\Gamma_0} \int\limits_0^{+\infty} \int\limits_0^{+\infty} f\left(a,x,y\right) P\left(a,y\right) dy da. \end{cases} \tag{12}$$

Of course this system can be reduced to a single equation on P, and λ depends continuously upon $\tilde{G}$. For a pure age-structured model it can be solved by the method of characteristics.

For further purposes, it is also useful to introduce the adjoint system following the principles of the GRE method. The adjoint problem reads:

$$\begin{cases} \lambda\varphi - \Gamma_0 \dfrac{\partial \varphi}{\partial a} - \Gamma_1\left(a,x\right) \dfrac{\partial \varphi}{\partial x} - 2\displaystyle\int_0^{+\infty} \varphi\left(0,y\right) f\left(a,y,x\right) dy \\ \qquad\qquad = -\left(L\left(a,x\right) + F(a,x) + d_1\right) \varphi + L\left(a,x\right) \psi, \\ \left(\lambda + \tilde{G} + d_2\right) \psi = \tilde{G}\varphi, \end{cases} \tag{13}$$

φ and ψ being positive and normalised by the condition:

$$\int_0^{+\infty}\int_0^{+\infty}[\varphi(a,x)P(a,x)+\psi(a,x)Q(a,x)]dadx=1.$$

These equations imply that solutions of (11) satisfy the "conservation law":

$$\begin{aligned}\int_0^{+\infty}\int_0^{+\infty}[\varphi(a,x)p(t,a,x)+ &\quad \psi(a,x)q(t,a,x)]dadx\\ &= e^{\lambda t}\int_0^{+\infty}\int_0^{+\infty}[\varphi(a,x)p_i(a,x)+\psi(a,x)q_i(a,x)]dadx,\end{aligned}$$

which clearly expresses exponential growth with rate λ.

In the following, we explain why these growth rates can allow to qualitatively distinguish between healthy and tumoral tissues. This is made possible by considering the behaviour of the first eigenvalue λ for the system linearised at the extreme values of the recruitment function G. We present the main features of the nonlinear problem using a method introduced in [11] enforcing conditions on the linearised problem. In particular, the linearised adjoint problem serves to compute the weights measuring the growth of the system. This imposes to assume several comparisons between these weights and the quantities (φ^*,ψ^*) measuring the quantity N in (5) (see H2, H4, H6... below). These assumptions are always fulfilled when a and x remain *a priori* bounded because the weights are all positive and bounded, as a consequence of the Krein-Rutman theorem. In the non-compact cases at hand, these conditions are more restrictive and it is difficult to analyse the behavior or (φ,ψ) for large a (see [29,33,34] for results in this direction). But our numerical tests have always confirmed the theoretical predictions even though we did not compute the solutions to the adjoint problem (see Section 4).

2.2. Analysis for a healthy tissue

Coming back to the nonlinear problem, we give conditions on the linearised problem enforcing homeostasis for healthy tissue. These are given in separate paragraphs where we prove firstly non-extinction, and then *a priori* bounds and existence of a steady state.

2.2.1. Non-extinction (*a priori* bound from below)

We first state conditions enforcing non-extinction. For this purpose, we need to investigate the linearised problem around $N(t)=0$ and its first eigenvalue.
We assume that the coefficients are such that the following qualitative properties hold true:

(H1) For $\tilde{G}=G(0)=\alpha_1$, the first eigenvalue, denoted here as λ_0, of system (12) and its corresponding adjoint system (13), is positive ($\lambda_0>0$).
(H2) For the corresponding solutions to (12) and (13) obtained for $\tilde{G}=G(0)$, (p_0,q_0) and (φ_0,ψ_0), there exists a positive constant C_0, such as $\varphi^*\leq C_0\varphi_0$ and $\psi^*\leq C_0\psi_0$ ($\varphi^* and \psi^*$ being as defined in equation (5)).

These assumptions express that even if there are very few cells in the healthy tissue, the population can be regenerated spontaneously. As mentioned earlier, if we *a priori* assume the existence of a maximum possible age, then the positivity of φ_0 and ψ_0 implies that (H2) is automatically satisfied for any pair of bounded functions (φ^*, ψ^*).

Proposition 2.1 *Under hypotheses (H1)–(H2) and*

$$0 < \int_0^{+\infty}\int_0^{+\infty} [\varphi_0(a,x)p_i(a,x) + \psi_0(a,x)q_i(a,x)]dadx < \infty,$$

there exists a real number m_0 such that

$$(\forall t \geq 0) \qquad \int_0^{+\infty}\int_0^{+\infty} [\varphi_0(a,x)p(t,a,x) + \psi_0(a,x)q(t,a,x)]dadx \geq m_0 > 0.$$

Proof of Proposition 2.1. We define the quantity

$$S_0(t) = \int_0^{+\infty}\int_0^{+\infty} [\varphi_0(a,x)p(t,a,x) + \psi_0(a,x)q(t,a,x)]dadx.$$

Using (11) and (13), we have by straightforward computation:

$$\begin{aligned}
\frac{dS_0}{dt}(t) &= \lambda_0 S_0(t) + (G(0) - G(N(t))) \int_0^{+\infty}\int_0^{+\infty} [\psi_0(a,x) - \varphi_0(a,x)]q(t,a,x)dadx \\
&= \lambda_0 S_0(t) - \frac{\lambda_0 + d_2}{G(0)}(G(0) - G(N(t))) \int_0^{+\infty}\int_0^{+\infty} \psi_0(a,x)q(t,a,x)dadx \\
&\geq \lambda_0 S_0(t) - \frac{\lambda_0 + d_2}{G(0)}(G(0) - G(N(t)))S_0(t),
\end{aligned}$$

because φ_0, ψ_0 and p are positive and G is decreasing. Hence we arrive at

$$\frac{dS_0}{dt}(t) \geq \left(\frac{\lambda_0 + d_2}{G(0)}G(N(t)) - d_2\right) S_0(t).$$

Therefore, firstly,

$$S_0(t) \geq S_0(0) \exp\left\{\int_0^t \left(\frac{\lambda_0 + d_2}{G(0)}G(N(t)) - d_2\right) dt\right\} > 0.$$

Now, either the minimum of $S_0(t)$ is attained at $t = 0$ and $S_0(t) \geq S_0(0)$, or it is attained at some point t_0 (possibly at infinity) where $\frac{dS_0}{dt}(t_0) = 0$, which gives

$$G(N(t_0))\frac{\lambda_0 + d_2}{G(0)} - d_2 \leq 0,$$

or equivalently

$$G(N(t_0)) \leq \frac{d_2}{\lambda_0 + d_2} G(0).$$

Since G is continuous and decreasing to 0, there exists a number $N_0 > 0$ such that

$$G(N_0) = \frac{d_2}{\lambda_0 + d_2} G(0).$$

Thus $G(N(t_0)) \leq G(N_0)$ which implies that $N(t_0) \geq N_0 > 0$ and $S_0(t) \geq S_0(t_0) \geq \dfrac{N_0}{C_0} > 0$ for all $t \geq 0$, by (H2). Therefore we have proved the result with

$$m_0 = \min\left(\frac{N_0}{C_0}, S_0(0)\right).$$

□

2.2.2. Limited growth (*a priori* bound from above)

We also need conditions enforcing tissue homeostasis, meaning that the total cell population density is limited in its growth: for this purpose we assume that for some $\lambda_{\lim} < 0$, there are $N_{\lim} > 0$ and nonnegative functions $(\varphi_{\lim}, \psi_{\lim})$ satisfying:

(H3) For $\tilde{G} = G(N_{\lim}) = \dfrac{\alpha_1 \theta^n}{\theta^n + N_{\lim}^n}$, the first eigenvalue, denoted here as $\lambda_{\lim}$ of system (12) and its adjoint(13), is negative ($\lambda_{\lim} < 0$).
(H4) For the corresponding solutions to (12) and (13) obtained for $\tilde{G} = G(N_{\lim})$, $(p_{\lim}, q_{\lim})$ and $(\varphi_{\lim}, \psi_{\lim})$, there exists a positive constant $C_{\lim}$, such that $\varphi^* \geq C_{\lim}\varphi_{\lim}$ and $\psi^* \geq C_{\lim}\psi_{\lim}$.

These assumptions express that a large excess of cells is regulated negatively and thus the population remains bounded as we state it now.

Proposition 2.2 *Under hypotheses (H3) and (H4) and*

$$0 < \int_0^{+\infty}\int_0^{+\infty} [\varphi_{\lim}(a,x)p_i(a,x) + \psi_{\lim}(a,x)q_i(a,x)]dadx < \infty,$$

there is a number $m_{\lim}$ such that

$$(\forall t \geq 0) \qquad \int_0^{+\infty}\int_0^{+\infty} [\varphi_{\lim}(a,x)p(t,a,x) + \psi_{\lim}(a,x)q(t,a,x)]dadx \leq m_{\lim}.$$

Proof of Proposition 2.2. As in the proof of Proposition 2.1, we define the auxilliary quantity

$$S_{\lim}(t) = \int_0^{+\infty}\int_0^{+\infty} [\varphi_{\lim}(a,x)p(t,a,x) + \psi_{\lim}(a,x)q(t,a,x)]dadx.$$

Then, we compute

$$\begin{aligned}\frac{dS_{\lim}}{dt}(t) &= \lambda_{\lim}S_{\lim}(t) - \frac{\lambda_{\lim}+d_2}{G(N_{\lim})}\left(G(N_{\lim}) - G(N(t))\right)\int_0^{+\infty}\int_0^{+\infty}\psi_{\lim}(a,x)q(t,a,x)dadx \\ &\leq \lambda_{\lim}S_{\lim}(t) - \frac{\lambda_{\lim}+d_2}{G(N_{\lim})}\left(G(N_{\lim}) - G(C_{\lim}S_{\lim}(t))\right)\int_0^{+\infty}\int_0^{+\infty}\psi_{\lim}(a,x)q(t,a,x)dadx,\end{aligned}$$

because, due to assumption (H4)

$$N(t) \geq C_{\lim}S_{\lim}(t).$$

Therefore, following the arguments above, we arrive at the estimate

$$S_{\lim}(t) \leq \sup\left(S_{\lim}(0), \frac{N_{\lim}}{C_{\lim}}\right) := m_{\lim},$$

which concludes the proof of Proposition 2.2. □

2.2.3. Steady state for a healthy tissue

Numerical experiments show that in the case of healthy tissues, the cell population goes to a steady state that represents tissue homeostasis. Even though the existence of a unique steady state can be analysed in the present model, the convergence toward this steady state is an open question.

Such a steady state (p^*, q^*) of (1), is the solution to the system of equations:

$$\begin{cases} \dfrac{\partial\left(\Gamma_0 p^*\right)}{\partial a} + \dfrac{\partial\left(\Gamma_1(a,x)\,p^*\right)}{\partial x} = -\left(L(a,x) + F(a,x) + d_1\right)p^*(a,x) + G\left(N^*\right)q^*(a,x), \\ L(a,x)\,p^*(a,x) - \left(G\left(N^*\right) + d_2\right)q^*(a,x) = 0, \\ p^*(0,x) = \dfrac{2}{\Gamma_0}\displaystyle\int_0^{+\infty}\int_0^{+\infty} f(a,x,y)p^*(a,y)\,dady, \end{cases} \tag{14}$$

with

$$N^* = \int_0^{+\infty}\int_0^{+\infty}[\varphi^*(a,x)p^*(a,x) + \psi^*(a,x)q^*(a,x)]dadx. \tag{15}$$

Proposition 2.3 *With the assumptions (H1), (H2), (H3) and (H4), the system (14), (15) has a unique positive solution* (p^*, q^*).

Proof of Proposition 2.3. When N^* is given, equation (14) is equivalent to say that the system (12) as the eigenvalue $\lambda = 0$. To prove that this can be achieved, to a state

population number N^*, we associate $\lambda(N^*)$, the first eigenvalue to the problem in (p, q)

$$\begin{cases} \lambda(N^*)p + \dfrac{\partial\left(\Gamma_0 p\right)}{\partial a} + \dfrac{\partial\left(\Gamma_1\left(a,x\right)p\right)}{\partial x} = -\left(L\left(a,x\right) + F(a,x) + d_1\right)p\left(a,x\right) + G\left(N^*\right)q\left(a,x\right), \\ \lambda(N^*)q + \left(G\left(N^*\right) + d_2\right)q\left(a,x\right) = L\left(a,x\right)p\left(a,x\right), \\ p\left(0,x\right) = \dfrac{2}{\Gamma_0}\displaystyle\int_0^{+\infty}\int_0^{+\infty} f(a,x,y)p\left(a,y\right)\,dady, \end{cases}$$

On the one hand, we know by (H1), (H2) that $\lambda(0) > 0$ and by (H3) and (H4) that $\lambda(N_{\lim}) < 0$. On the other hand, $N^* \mapsto \lambda(N^*)$ is continuous (by usual perturbation theory since G is continuous), and it is decreasing since G is decreasing with N^*. To see this, we can rewrite the system on (p, q) as

$$\lambda(N^*)p + \frac{\partial\left(\Gamma_0 p\right)}{\partial a} + \frac{\partial\left(\Gamma_1\left(a,x\right)p\right)}{\partial x} = -\left(F(a,x) + d_1\right)p\left(a,x\right) - \frac{L(a,x)\big(\lambda(N^*) + d_2\big)}{\lambda(N^*) + G(N^*) + d_2}p,$$

and notice that the function

$$(\lambda, G) \mapsto \lambda + \frac{L(a,x)\big(\lambda + d_2\big)}{\lambda + G + d_2}$$

is decreasing in G and increasing in λ.

From the monotonicity property of the function $\lambda(N^*)$ and its values at 0 and ∞, we deduce that there is a unique value of N^* such that $\lambda(N^*) = 0$.

It remains to normalise the corresponding eigenvectors (p, q) properly (by multiplication) to obtain (15) and thus a solution to (14)–(15). □

2.3. Analysis for a tumoral tissue

For the tumoral case, the recruitment function from quiescence to proliferation is given by the function:

$$G\left(N\right) = \frac{\alpha_1\theta^n + \alpha_2 N^n}{\theta^n + N^n}.$$

for which $G(\infty) := \lim_{t\longrightarrow+\infty} G(t) = \alpha_2 > 0$, a situation fundamentally different from the healthy tissue case in which homeostasis requires $G(\infty) = 0$.

Here, we expect that the population shows unlimited growth, and we give conditions leading to this property.

2.3.1. Exponential growth

The following conditions on the linearised problem enforce exponential growth for the tumoral tissue case:

(H5) For $\tilde{G} = G(\infty) = \alpha_2$, the first eigenvalue, denoted here as λ_1 of system (12) and its adjoint (13), is strictly positive ($\lambda_1 > 0$).
(H6) For the corresponding solutions to (12) and (13) obtained for $\tilde{G} = G(\infty)$, (p_1, q_1), (φ_1, ψ_1), there exists a positive constant C_1, such that $\varphi^* \geq C_1\varphi_1$ and $\psi^* \geq C_1\psi_1$.

Proposition 2.4 *Under hypotheses (H5) and (H6), there exists a positive constant M such that:*

$$N(t) \geq Me^{\lambda_1 t}.$$

Proof of Proposition 2.4. Let us define the quantity

$$S_1(t) = \int_0^{+\infty}\int_0^{+\infty} [\varphi_1(a,x)p(t,a,x) + \psi_1(a,x)q(t,a,x)]dadx.$$

We have, since G is decreasing,

$$\begin{aligned}\frac{dS_1}{dt}(t) &= \lambda_1 S_1(t) + \frac{\lambda_1 + d_2}{G(\infty)}\left(G(N(t)) - G(\infty)\right)\int_0^{+\infty}\int_0^{+\infty}\psi_1(a,x)q(t,a,x)dadx \\ &\geq \lambda_1 S_1(t).\end{aligned}$$

This implies that $S_1(t)$ has exponential growth, i.e., $S_1(t) \geq S_1(0)e^{\lambda_1 t}$. Finally, thanks to (H6) we have $N(t) \geq C_1 S_1(t)$. We conclude that $N(t) \geq C_1 S_1(0)e^{\lambda_1 t}$ and Proposition 2.4 is proved with $M = C_1 S_1(0)$. □

2.3.2. Subpolynomial growth

We are now interested in the case when the total (weighted) cell population density $N(t)$ has unlimited growth, i.e., $\lim_{t\longrightarrow+\infty} N(t) = +\infty$, but not exponential growth and we look for conditions giving polynomial growth. We are not able to prove such a behaviour but only subpolynomial growth (in the next paragraph we prove unlimited growth). For this purpose we assume the following hypotheses:

(H7) For $\tilde{G} = G(\infty) = \alpha_2$, the first eigenvalue of system (12) and its adjoint (13) is $\lambda_1 = 0$.
(H8) For the corresponding solutions to (12) and (13) obtained for $\tilde{G} = G(\infty)$, (p_2, q_2), (φ_2, ψ_2), there exists positive constants C_2 and C_3, such that $C_3\varphi_2 \leq \varphi^* \leq C_2\varphi_2$ and $C_3\psi_2 \leq \psi^* \leq C_2\psi_2$.

Proposition 2.5 *Under hypotheses (H7) and (H8), there exists a positive constant C such that for large t,*

$$N(t) \leq Ct^{1/n}.$$

Proof of Proposition 2.5. As in the proof of Proposition 2.4, we define:

$$S_2(t) = \int_0^{+\infty}\int_0^{+\infty} [\varphi_2(a,x)p(t,a,x) + \psi_2(a,x)q(t,a,x)]dadx.$$

Since by $(H7)$, we have $\lambda_1 = 0$, then (as in the proof of the previous proposition):

$$\frac{dS_2}{dt}(t) = \frac{d_2}{G(\infty)}\left(G(N(t)) - G(\infty)\right)\int_0^{+\infty}\int_0^{+\infty}\psi_2(a,x)q(t,a,x)dadx,$$

which proves in the first place, since G is decreasing, that

$$\frac{dS_2}{dt}(t) \leq \frac{d_2}{G(\infty)}\left(G(N(t)) - G(\infty)\right) S_2(t).$$

But since

$$G(N) - G(\infty) = \frac{(\alpha_1 - \alpha_2)\theta^n}{\theta^n + N^n},$$

and because $N(t) \geq C_3 S_2(t)$ thanks to (H8), we obtain

$$\frac{dS_2}{dt}(t) \leq \frac{d_2}{G(\infty)} \frac{(\alpha_1 - \alpha_2)\theta^n S_2(t)}{\theta^n + (C_3 S_2(t))^n}. \tag{16}$$

On the other hand, let us consider the function $\Sigma(t) = a(t + t_0)^{1/n}$ with $t_0 > 0$: For $\frac{a^n}{n} \geq \frac{d_2}{G(\infty)} \frac{(\alpha_1 - \alpha_2)\theta^n}{C_3^n}$, $\Sigma(t)$ is a supersolution to (16) because

$$\begin{aligned}
\frac{d\Sigma}{dt}(t) &= \frac{a}{n}(t + t_0)^{1/n-1} \\
&= \frac{a^n}{n}\left[\Sigma(t)\right]^{1-n} \\
&\geq \frac{d_2}{G(\infty)} \frac{(\alpha_1 - \alpha_2)\theta^n \Sigma(t)}{\theta^n + (C_3\Sigma(t))^n}.
\end{aligned}$$

Henceforth, for t_0 large enough to ensure $\Sigma(0) \geq S_2(0)$, we have by the comparison principle

$$S_2(t) \leq \Sigma(t).$$

¿From this inequality, using $(H8)$, we obtain,

$$N(t) \leq C_2 \Sigma(t),$$

which proves the proposition. □

Remark 2.6 *A motivation for (H7) is that one cannot exclude that actual tumours grow neither exponentially nor with saturation behaviour. Indeed, experimental observations [9] and numerical simulations with spatial models [15] show cases when $N(t) \approx t^3$. In these cases we can infer that a reasonable choice for parameter n, in the recruitment function G defined through (6), is $n = \frac{1}{3}$. The interpretation of this unlimited polynomial behaviour is then simple for tumour spheroids (in which average cell number is assumed to be proportional to the tumour volume): from the differential inequality for $S_2(t)$ we have*

$$\frac{dS_2}{dt}(t) \simeq S_2^{\frac{2}{3}}(t), \tag{17}$$

which may account for an effect of surfacic pressure on the tumour volume, i.e., a growth limit that is proportional to the outer rim cell population of the spheroid.

2.3.3. Unlimited growth

We are now interested in the case when λ_1, the first eigenvalue corresponding to $N = \infty$, vanishes as in (H7). Then we can still prove a result implying unlimited growth. We use the assumption

(H9) for all $N < \infty$, the eigenvalue $\lambda(N)$ corresponding to $\tilde{G} = G(N)$ in system (12) and its adjoint (13) satisfies $\lambda(N) > 0$
(H10) there is a 'uniform' constant C_u such that any of the solutions (φ_N, ψ_N) to the adjoint problem satisfy $\varphi^* \geq C_u \varphi_N$, $\psi^* \geq C_u \psi_N$.

Of course, compatibility with (H7) imposes that $\lambda(N) \to 0$ as $N \to \infty$ which is the interesting case. Recall also that $\lambda(N)$ is a non-increasing function of N.

Proposition 2.7 *Under hypotheses (H9)and (H10), we have:*

$$\lim_{t\to\infty} N(t) = \infty.$$

Proof of Proposition 2.7. As a **first step**, we prove that $\limsup_{t\to\infty} N(t) = \infty$. Assume by contradiction that for some ν, $\limsup N(t) < \nu < \infty$. As usual, we define the auxiliary quantity

$$S_\nu(t) = \int_0^{+\infty}\int_0^{+\infty} [\varphi_\nu(a,x)p(t,a,x) + \psi_\nu(a,x)q(t,a,x)]dadx.$$

It satisfies, as in Proposition 2.4, and for t large enough

$$\begin{aligned} \frac{dS_\nu}{dt}(t) &= \lambda(\nu)S_\nu(t) + \frac{\lambda(\nu)+d_2}{G(\nu)}\left(G(N(t)) - G(\nu)\right)\int_0^{+\infty}\int_0^{+\infty}\psi_\nu(a,x)q(t,a,x)dadx \\ &\geq \lambda(\nu)S_\nu(t). \end{aligned}$$

This proves that $S_\nu(t) \to \infty$ as $t \to \infty$ (because $\lambda(\nu) > 0$ by (H9)). But from (H10), we have $N(t) \geq C_u S_\nu(t)$ which contradicts the existence of such a ν and concludes the first step.

In the **second step**, we prove that $\lim_{t\to\infty} N(t) = \infty$. To do that we choose $\nu = \infty$ in the previous step and obtain, because $\lambda(\infty) = \lambda_1 = 0$,

$$\frac{dS_\infty}{dt}(t) = \frac{\lambda(\infty)+d_2}{G(\infty)}\left(G(N(t)) - G(\infty)\right)\int_0^{+\infty}\int_0^{+\infty}\psi_\nu(a,x)q(t,a,x)dadx > 0.$$

Therefore $S_\infty(t)$ is increasing. But its limit as $t \to \infty$ can only be infinity because by the first step, its *limsup* is infinity. Finally, using again (H10), we have $N(t) \geq C_u S_\infty(t)$ and the result is proved. □

3. Numerical scheme

We now present the numerical simulation of the molecular structured population model (1). For the transport equation, it is natural to use a finite volume discretisation. The main advantage is that, at the discrete level, we can keep the basic local conservation law expressed by the divergence nature of the differential terms. The finite volume method relies on well established theories and properties that one can find, for instance, in the textbooks [10,16,17,24].

Before we present the numerical scheme, we need to introduce some notations. We use a rectangular grid in age a and cyclin content x, and we set

- $\Delta a,\ \Delta x$ are the uniform mesh sizes, Δt is the time step,
- $t_k = k\Delta t$,
- $a_i = (i-\frac{1}{2})\Delta a,\ a_{i+\frac{1}{2}} = (i-1)\Delta a, \qquad 1 \le i \le I_M$, with $I_M\Delta a$ the maximum numerical age encountered,
- $x_j = (j-\frac{1}{2})\Delta x,\ x_{j+\frac{1}{2}} = (j-1)\Delta x, \qquad 1 \le j \le J_M$, with $J_M\Delta x \approx x_{\max}$,
- $C_{i,j}$ is the cell $[a_{i-\frac{1}{2}}, a_{i+\frac{1}{2}}] \times [x_{j-\frac{1}{2}}, x_{j+\frac{1}{2}}]$.

The motivation of these notations for the grid points $a_{i+\frac{1}{2}}$ and $x_{j+\frac{1}{2}}$ comes from the principle of the finite volume method which is to approximate the averaged quantities

$$p_{i,j}^k = \frac{1}{\Delta x\ \Delta a}\ \int_{C_{i,j}} p(t_k,a,x)da\ dx, \qquad q_{i,j}^k = \frac{1}{\Delta x\ \Delta a}\ \int_{C_{i,j}} q(t_k,a,x)da\ dx.$$

These quantities satisfy a discrete version of the continuous equations (1) which allow us to compute recursively the states at time t_{k+1} from the state at time t_k:

$$\begin{cases} p_{i,j}^{k+1} - p_{i,j}^k + \frac{\Delta t}{\Delta a}\left[\mathcal{F}_{i+\frac{1}{2},j}^k - \mathcal{F}_{i-\frac{1}{2},j}^k\right] + \frac{\Delta t}{\Delta x}\left[\mathcal{G}_{i,j+\frac{1}{2}}^k - \mathcal{G}_{i,j-\frac{1}{2}}^k\right] = \Delta t\ G^k q_{i,j}^k - \Delta t\ [L_{i,j} + F_{i,j} + d_1]p_{i,j}^k, \\ \\ q_{i,j}^{k+1} - q_{i,j}^k = \Delta t\ L_{i,j}\ p_{i,j}^k - \Delta t\ [G^k + d_2]q_{i,j}^k. \end{cases} \tag{18}$$

The various coefficients arising in this system have to be approximated and we use a first order scheme. We begin with the source terms; the coefficient $L_{i,j}$ can be chosen as the point values at (a_i, x_j) of the functions L, and we take

$$G^k = G(N^k), \qquad N^k = \Delta x\ \Delta a\ \sum_{i,j}\left[\varphi_{i,j}^* p_{i,j}^k + \psi_{i,j}^* q_{i,j}^k\right]. \tag{19}$$

The last coefficients, $F_{i,j}$, are related to the boundary fluxes and are given below.

Regarding the fluxes $\mathcal{F}$, $\mathcal{G}$ we choose standard upwind schemes which are particularly easy because the 'velocities' have a positive sign, for $1 \le i \le I_M$, $1 \le j \le j_M$, we set

$$\mathcal{F}_{i+\frac{1}{2},j}^k = \Gamma_0\ p_{i-1,j}^k, \qquad \mathcal{G}_{i,j+\frac{1}{2}}^k = \Gamma_1(a_i, x_{j+\frac{1}{2}})\ p_{i,j-1}^k. \tag{20}$$

The missing fluxes (labels $i = 1$ and $j = 1$, fluxes on the left and down) correspond to the cell division boundary conditions,

$$\mathcal{F}^k_{\frac{1}{2},j} = 2\Delta x\ \Delta a\ \sum_{i,k} f_{i,j,k}\ p^k_{i,k}, \qquad \mathcal{G}^k_{i,\frac{1}{2}} = 0, \tag{21}$$

where we have denoted again by $f_{i,j,k}$ the point value of the renewal function $f(a, x, y)$ at the points a_i, x_i, and x_k. Therefore, we can derive also the coefficients, $F_{i,j}$:

$$F_{i,j} = \Delta x\ \Delta a\ \sum_{i,k} f_{i,k,j}. \tag{22}$$

We recall that these schemes have been widely studied in the references mentioned above and that, as always for explicit schemes, their stability is subject to a limitation on the time step Δt, called CFL (Courant, Friedrichs, Levy) condition (here all the "max" are taken over $1 \le i \le I_M$ and $1 \le j \le J_M$)

$$\begin{cases} \Delta t\ \left[\dfrac{\Gamma_0}{\Delta a} + \dfrac{\max\ \Gamma_1(a_i, x_{j+\frac{1}{2}})}{\Delta x} + \max(L_{i,j} + F_{i,j}) + d_2\right] \le 1, \\ \\ \Delta t\ [G^k + d_2] \le 1. \end{cases} \tag{23}$$

In practice, some terms can be discretised with an implicit scheme, a method which improves the time steps thanks to a better CFL condition. In the numerical results presented below, we have used a fully implicit scheme for the apoptosis, demobilisation, gain and boundary terms.

Another fundamental property of this finite volume method is that it reproduces at the discrete level the balance laws expressed by the continuous equation. Namely, we have

$$\sum_{i,j}[p^{k+1}_{i,j} + q^{k+1}_{i,j}] = \sum_{i,j}[p^k_{i,j} + q^k_{i,j}] + \frac{\Delta t}{2}\sum_i \mathcal{F}^k_{\frac{1}{2},j} - \Delta t\ \sum_{i,j}[d_1 p^k_{i,j} + d_2 q^k_{i,j}]$$

This follows from the addition of the two equalities in (18), from the cancellations between terms arising in the equations on p^{k+1} and q^{k+1}, and from the cancellations between the flux term $\mathcal{F}^k_{\frac{1}{2},j}$, in (21), and the term $F_{i,j}p^k_{i,j}$, thanks to definition (22).

4. Numerical validation

Parameters	Values		Parameters	Values
c_1	0.1		A^*	23 $(hours)$
c_2	0.075		A_1	4 $(hour^{-1})$
c_3	1.2		A_2	2
c_4	0.4 $(hour^{-1})$		γ_2	5
w_1	1.95		$\overline{A}$	18 $(hours)$
Γ_0	1		α_1	8 $(hour^{-1})$
k_1	1.2 $(hour^{-1})$		θ	1
k_2	1.5		α_2	.4797 $(hour^{-1})$
d_1	0		γ_1	5
d_2	.02 $(hour^{-1})$		n (usual case)	1/3

Table 1. Parameters and values used in simulations.

Some of the model parameters are known for specific cells in other settings for functions used in a similar context, [27,40,6,43,25,22] and are used in [8]. Here, our aims are to exhibit the numerical differences between solutions for the two boundary conditions (8) and (9), and to exhibit the polynomial growth, when $\lambda_1 = 0$, according to Proposition 2.5. Therefore, we have made realistic choices of a range of values within which our numerical simulations exhibit a behaviour illustrating the theoretical properties of the model demonstrated under the various assumptions $(H1)$ to $(H10)$, but we have not chosen the parameters among the above literature because we do not aim at covering a specific organ. These are given in Table 1. Notice that the parameter θ is simply a choice of the unit for number of cells and can be taken to be 1 without lose of generality. Our parameters also lead to $x_{\max} = 3$ which fixes a unit for x. They are given for the boundary condition (8) of uniform repartition of x at birth. In our numerical simulations we have used $\varphi^* = \psi^* \equiv 1$, i.e., we have assumed that all cells are eligible for recruitment control (by cell density inhibition, growth or antigrowth factors) in phase G_1. We have used 60 grid points for the x variable and 80 for the age variable.

Figure 1 shows the trend to a steady state as stated in Proposition 2.3 and Figure 2 shows the distribution of cells according to their age and *cyclin D/(CDK4 or 6)* concentrations in the proliferative phase in the case of uniform cyclin complex after division, i.e., the function f given by (8). Figure 3 presents the same result for the case of equal repartition (9). We have also verified that assumptions (H1) and (H3) hold true for a healthy tissue. The so-called power algorithm [17] allows us to obtain numerically the first eigenvalue of system (12). In order to perform the computation of Figure 5, a high accuracy on the approximation $\lambda_1 = 0$ is needed, this has led us to compute more digits on $\alpha_2 = .47972513897$.

The time evolution of the total number of quiescent and proliferative cells is shown in figure 4 in the case of a polynomial growth when $\lambda_1 = 0$ with $n = 1/3$ in a normal scale where it is difficult to guarantee a polynomial growth. Therefore we show, in Figure 5 (left), different cases where the Malthus coefficient λ_1 is zero, with $n = 1$, $n = \frac{1}{2}$, $n = \frac{1}{3}$ in the recruitment function G defined by (6). We can see on this log-log scale plot of the total cell number $N(t)$ as a function of time t that for large t, $N(t) \approx t^{1/n}$, i.e., the tumour

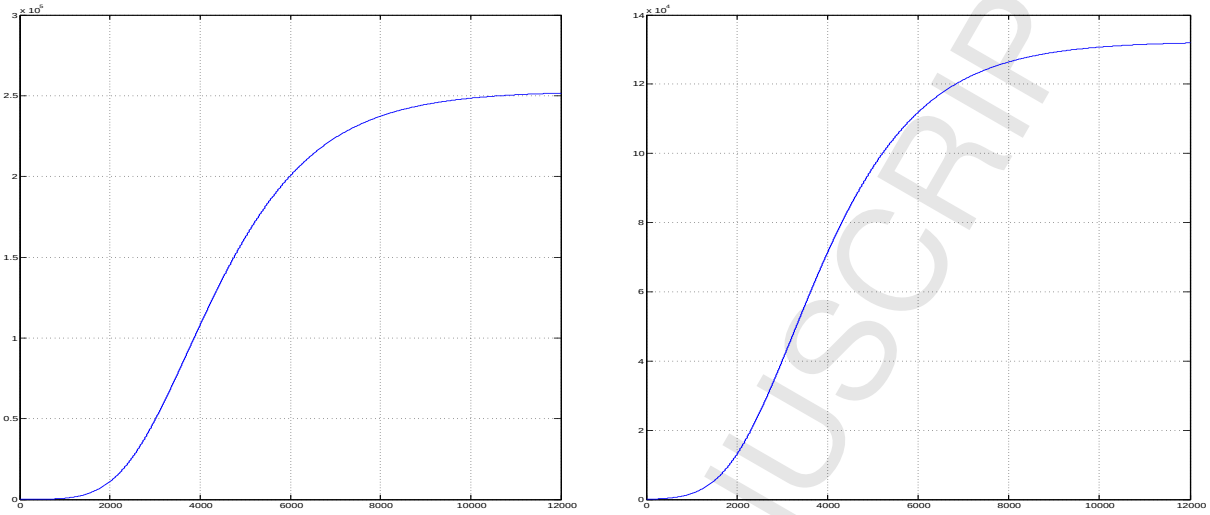

Figure 1. Evolution of the total cell population for a healthy tissue. Left: total quiescent cells $\int_0^{+\infty}\int_0^{+\infty} q(t,a,x)dadx$; right: total proliferating cells $\int_0^{+\infty}\int_0^{+\infty} p(t,a,x)dadx$.

shows unlimited polynomial growth depending upon n as it is foreseen by Proposition 2.5. On the right we have depicted the exponential growth (in a log scale) when $\lambda_1 > 0$. Then the value of n does not determine the exponential growth, in accordance with Proposition 2.4.

REFERENCES

1. Adimy, M., Crauste, F., Pujo-Menjouet, L. On the stability of a nonlinear maturity structured model of cellular proliferation. Discrets and Continuous Dynamical Systems, 12(3):501-502 (2005).
2. Alberts, B., Bray, D., Lewis, J., Raff, M., Roberts, K., Watson, J.D. Molecular Biology of the Cell. Garland, New York (1994).
3. Arino, O. A survey of structured cell population dynamics. Acta Biotheor. 43:3-25 (1995).
4. Arino, O., Sanchez, E., Webb, G.F. Necessary and sufficient conditions for asynchronous exponential growth in age structured cell populations with quiescence. J. Math. Anal. Appl. 215:499-513 (1997).
5. Bagowski, C.P., Besser, J., Frey, C.R., Ferrell, J.E. The JNK cascade as a biochemical switch in mammalian cells: ultrasensitive and all-or-none responses. Curr. Biol. 13:315–320 (2003).
6. Blagosklonny, M.V., Pardee, A.B. The restriction point of the cell cycle. Cell Cycle, Mar-Apr 1(2):103-10 (2002).
7. Bekkal Brikci, F., Chiorino, G., Arino, O. G_1/S transition and cell population dynamics. *Submitted*.
8. Bekkal Brikci, F., Clairambault, J., Ribba, B., Perthame, B. An age-and-cyclin-structured cell population model with proliferation and quiescence. *Submitted*.

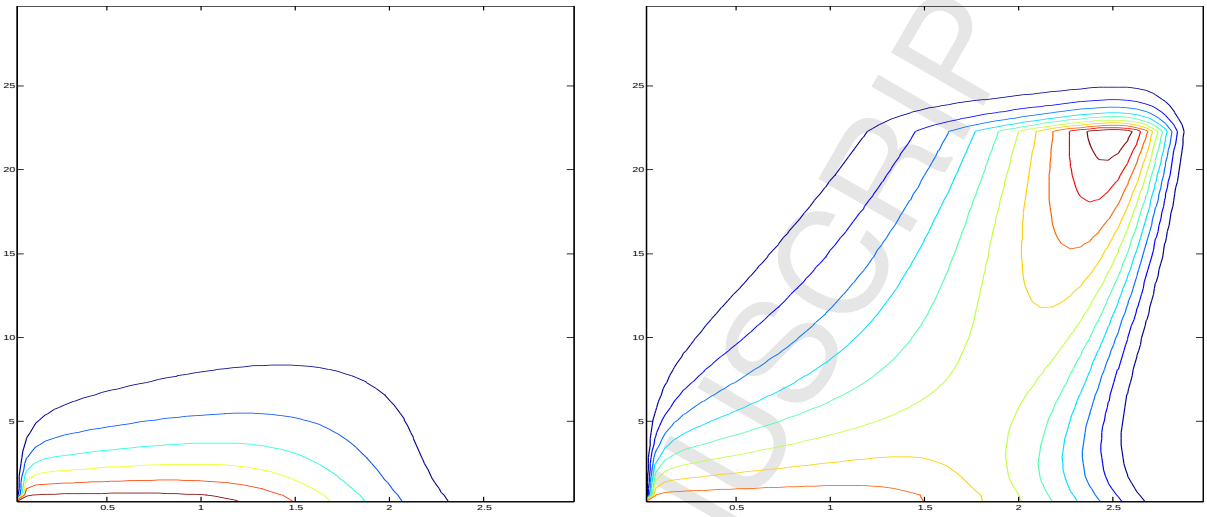

Figure 2. Isovalues of the total cell population for a healthy tissue at steady state (p^*, q^*): variable x (cyclin content) is in abscissae, variable a (age in the proliferating phase) in ordinates, and level lines indicate constant p^* or q^* values. Left: quiescent cells $q^*(a, x)$; right: proliferating cells $p^*(a, x)$.

9. Brú, A., Albertos, S., Subiza, J.L., Gareia-Asenjo, J.L., Brú,I. The universal dynamics of tumor growth. Biophys. J. 85:2948-2961 (2003).
10. Bouchut, F. Nonlinear stability of finite for volume methods for hyperbolic conservation laws and well-balanced schemes for sources. Series 'Frontiers in Mathematics', Birkhauser (2004).
11. Carrillo, J.A., Cuadrado, S., Perthame, B. Adaptive dynamics via Hamilton-Jacobi approach and entropy methods for a juvenile-adult model. Preprint Universitat Autonoma de Barcelona (2006).
12. Clairambault, J., Michel, P., Perthame, B. Circadian rhythm and tumour growth. C. R. Acad. Sci. (Paris), mathématique, 342(1):17-22 (2006).
13. Cooper, S. On the Proposal of a G0 phase and the restriction point. FASEB J. 12:367-373 (1998).
14. Dautray, R., Lions, J.-L. Mathematical analysis and numerical methods for sciences and technology, Springer, Ch VIII, pp. 187-199 (1990).
15. Drasdo, D., Höhme, S. A single-cell-based model of tumor growth in vitro: monolayers and spheroids. Phys Biol. Jul 12;2(3):133-47 (2005).
16. Godlewski, E., Raviart, P. Hyperbolic systems of conservation laws. Coll. SMAI Vol. 3/4, Ellipses, Paris (1991).
17. Golub, G. H., Van Loan, C.F. Matrix Computations. 3rd ed., Johns Hopkins University Press, Baltimore (1996).
18. Gyllenberg, M., Webb, G.F. A nonlinear structured population model of tumor growth with quiescence. J. Math. Biol. 28:671-694 (1990).
19. Gyllenberg, M., Webb, G.F. Age-size structure in populations with quiescence. Math.

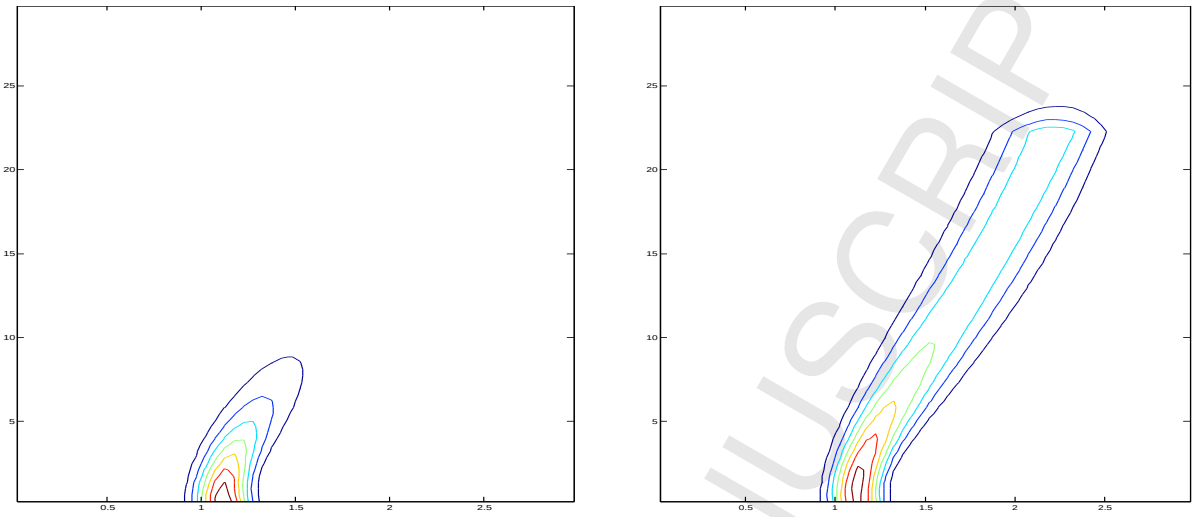

Figure 3. Same as Figure 2 but when division occurs with equal repartition of the complex *cyclin D/CDK(4 or 6)* along with the boundary condition (9). In this case two values are changed; $A_1 = .1$ and $\alpha_1 = 320$.

Biosciences 86 : 67-95 (1987).
20. Kimmel, M., Darzynkiewicz, Z., Arino, O., Traganos, F. Analysis of a cell cycle model based on unequal division of metabolic constituents to daughter cells during cytokinesis. J. Theor. Biol. 110:637-664 (1984).
21. Hartwell, L.H., Kastan, M.B. Cell cycle control and cancer. Science 266:1821-1828 (1994).
22. Hitomi, M., Stacey, D.W. Cellular ras and cyclin D1 are required during different cell cycle phases in cycling NIH 3T3 cells. Mol. Cell. Biol. 19(7):4623-32 (1999).
23. Kimmel, M., Darzynkiewicz, Z., Arino, O., Traganos, F. Analysis of a cell cycle model based on unequal division of metabolic constituents to daughter cells during cytokinesis. J. Theor. Biol. 110:637-664 (1984).
24. Leveque, R.J. Finite Volume Methods for Hyperbolic Problem. Cambridge Textbooks in Applied Mathematics (2002).
25. Lynch, J., Keller, M., Guo, R.J., Yang, D, Traber, P. Cdx1 inhibits the proliferation of human colon cancer cells by reducing cyclin D1 gene expression. Oncogene Sep 25;22(41):6395-407 (2003).
26. Mackey, M.C., Rudnicki, R. A new criterion for the global stability of simultaneous cell replication and maturation processes. J. Math. Biol. 38:195-219 (1999).
27. Foley, C., Bernard, S., Mackey, M.C. Cost-effective G-CSF therapy strategies for cyclical neutropenia: Mathematical modelling based hypotheses. J. Theor. Biol. 238:754–763 (2006).
28. Michel, P., Mischler, S., Perthame, B. General relative entropy inequality: an illustration on growth models, J. Math. Pures Appl. 84(9):1235-1260 (2005).
29. Michel, P. Existence of a solution to the cell division eigenproblem, Math. Mod. Meth.

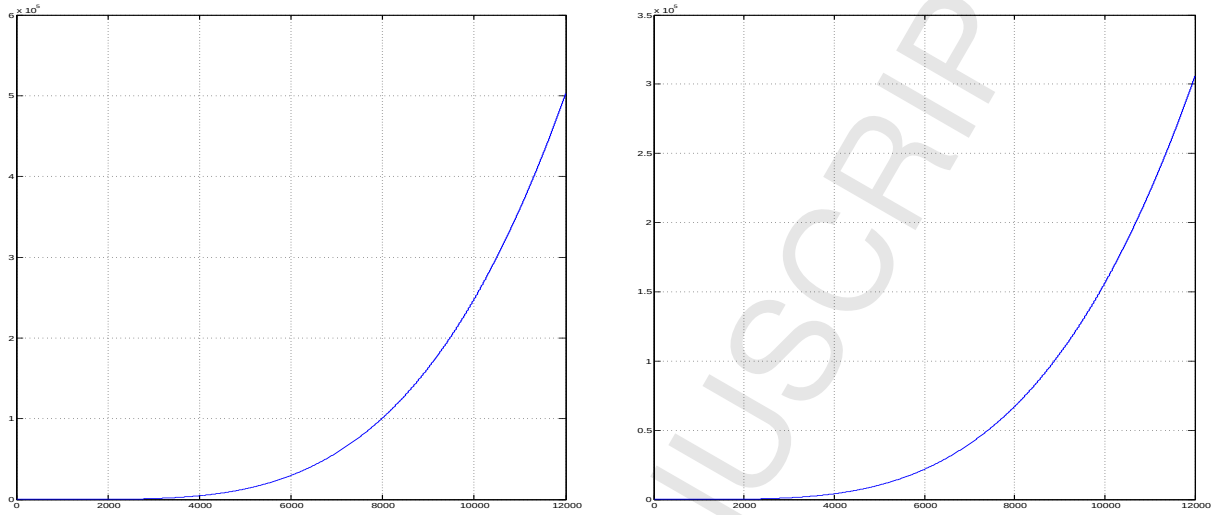

Figure 4. Evolution of the total cell population for a tumoral tissue with polynomial growth, $\lambda_1 = 0$, and $n = 1/3$. Left: total quiescent cells $\int_0^{+\infty}\int_0^{+\infty} q(t,a,x)dadx$; right: total proliferating cells $\int_0^{+\infty}\int_0^{+\infty} p(t,a,x)dadx$.

Appl. Sci, To appear in 2006.
30. Mischler, S., Perthame, B., Ryzhik, L. Stability in a nonlinear population maturation model, Math. Models Methods Appl. Sci., Vol. 12, No 12, pp.1751-1772, (2002).
31. Novak, B., Tyson, J.J. A model for restriction point control of the mammalian cell cycle. J. Theor. Biol. 230: 563-579 (2004).
32. Obeyesekere, M., Zimmerman, S.O. A Model of Cell Cycle Behavior Dominated by Kinetics of a Pathway Stimulated by Growth Factors. Bull. Math. Biol. 61:917–934 (1999).
33. Perthame, B. *Transport equations in biology*. 'Frontiers in mathematics'. Birkhauser (2006).
34. Perthame, B. Ryzhik, L. Exponential decay for the fragmentation or cell-division equation. J. Diff. Eq. 210 (2005) 155–177.
35. Qu, Z., Weiss, J.N., MacLellan, W.R. Regulation of the mammalian cell cycle: a model of the G1-to-S transition. Am. J. Physiol. Cell. Physiol. 284:349-364 (2003).
36. Rossa, B. Asynchronous exponential growth in a size structured cell population with quiescent compartment. Carcinogenesis and Cell & Tumor Growth. Arino et al. Ed., Volume 2, Chapter 14, pp. 183-200 (1995).
37. Sangfelt, O., Erickson, S., Castro, J., Heiden, T., Gustafsson, A., Einhorn, S., Grander, D. Molecular mechanisms underlying interferon-alpha-induced G0/G1 arrest: CKI-mediated regulation of G1 Cdk-complexes and activation of pocket proteins. Oncogene May 6; 18(18):2798-810 (1999).
38. Sherr, C.J., D-type cyclins. Trends Biochem. Sci. 20:187-190 (1995).
39. Stewart, E.J., Madden, R., Paul, G., Taddei, F., Aging and death in an organism that reproduces by morphologically symmetric division. PLoS Biol. 3(2):e45. Epub Feb 1

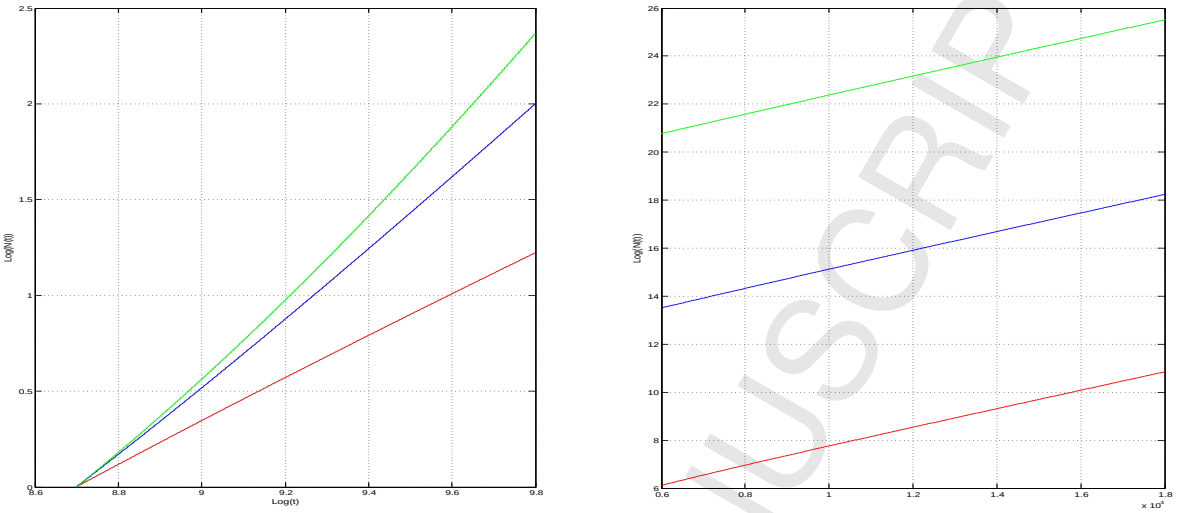

Figure 5. Evolution of the total cell population $\int_0^{+\infty}\int_0^{+\infty} q(t,a,x)dadx + \int_0^{+\infty}\int_0^{+\infty} p(t,a,x)dadx$ for a tumoral tissue with different values of $n = 1$ (lower curves), $n = 1/2$ (medium), $n = 1/3$ (upper). Left: with polynomial growth, $\lambda_1 = 0$, and a Log-Log scale (this shows the different power laws). Right: with exponential growth, $\lambda_1 > 0$, and a Log scale (this shows that n does not influence the exponential law).

(2005).

40. Swat, M., Kel, A., Herzel, H., Bifurcation analysis of the regulatory modules of the mammalian G1/S transition. Bioinformatics 20(10):1506-1511 (2004).
41. Val, J., Tyson, J., A purely deterministic model for the population dynamics of budding yeast. *Advances in Mathematical Population Dynamics - Molecules, Cells and Man*, Arino, O., Axelrod, D. & Kimmel, M. eds., World Scientific (1997).
42. Zetterberg, A., Larsson, O., Cell cycle progression and cell growth in mammalian cells: kinetic aspects of transition events. In Cell Cycle Control. Hutchinson, C., and Glover, D. M., eds, Oxford University Press, Oxford, New York, pp. 206-227 (1995).
43. Zwijsen, R.M., Klompmaker, R., Wientjens, E.B., Kristel, P.M., van der Burg, B., Michalides, R.J., Cyclin D1 triggers autonomous growth of breast cancer cells by governing cell cycle exit. Mol. Cell. Biol. Jun 16(6):2554-60 (1996).